Unconfounded Meta-analytical Frameworks for Multivariate Outcomes in Multigroup Observational Studies using Concordant Weights

Subharup Guha
Department of Biostatistics, University of Florida
and
David C. Christiani
Departments of Environmental Health and Epidemiology,
Harvard T.H. Chan School of Public Health
and
S. V. Subramanian
Departments of Sociology, Social and Behavioral Sciences, and
Harvard Center for Population and Development Studies,
Harvard T.H. Chan School of Public Health
and
Yi Li
Department of Biostatistics, University of Michigan

December 20, 2022

Abstract

While meta-analyzing retrospective cancer patient cohorts, an investigation of differences in the expressions of target oncogenes across cancer subtypes is of substantial interest because the results may uncover novel tumorigenesis mechanisms and improve screening and treatment strategies. Weighting methods facilitate unconfounded comparisons of multigroup potential outcomes in multiple observational studies. For example, Guha et al. (2022) introduced concordant weights, allowing integrative analyses of survival outcomes by maximizing the effective sample size. However, it remains unclear how to use this or other weighting approaches to analyze a variety of continuous, categorical, ordinal, or multivariate outcomes, especially when research interests prioritize uncommon or unplanned estimands suggested by post hoc analyses; examples include percentiles and moments of group potential outcomes and pairwise correlations of multivariate outcomes. This paper proposes a

unified meta-analytical approach accommodating various types of endpoints and fosters new estimators compatible with most weighting frameworks. Asymptotic properties of the estimators are investigated under mild assumptions. For undersampled groups, we devise small-sample procedures for quantifying estimation uncertainty. We meta-analyze multi-site TCGA breast cancer data, shedding light on the differential mRNA expression patterns of eight targeted genes for the subtypes infiltrating ductal carcinoma and infiltrating lobular carcinoma.

Keywords: Generalized balancing weights; Propensity score; Retrospective cohorts; Target population.

1 Introduction

It has been of substantial interest to investigate how the expression levels of oncogenes differ across cancer subtypes. For example, in a multi-site breast cancer study conducted at the Walter Reed National Military Medical Center, International Genomics Consortium, Memorial Sloan Kettering Cancer Center (MSKCC), Mayo Clinic, University of Pittsburgh, Roswell Park, and University of Miami, the focus was to discover how the mRNA expression of eight targeted breast cancer genes, namely, COL9A3, CXCL12, IGF1, ITGA11, IVL, LEF1, PRB2, and SMR3B (e.g., Zielińska & Katanaev 2020, Donzelli et al. 2020, Christopoulos et al. 2015) differ across infiltrating ductal carcinoma (IDC) and infiltrating lobular carcinoma (ILC); these disease subtypes respectively account for approximately 80% and 10% of all breast cancer cases in the United States (Wright 2022, Tran 2022). The results may help dissect disease subtype-specific mechanisms of tumorigenesis (Feng et al. 2018) and inform better screening and treatment strategies (Kumar et al. 2020).

The multistudy data are reposited at The Cancer Genome Atlas (TCGA) portal (NCI 2022), and include demographic, clinicopathological, and biomarker measurements; see the study-specific patient attributes summarized in Table 1. For each patient, the outcome is a multivariate vector consisting of mRNA expression measurements for the eight genes. We are interested in group comparisons and population-level summaries of disease subtype for these biomarkers, such as group comparison estimands (e.g., contrasts or correlations) and

marginal group summaries (e.g, means, standard deviations, and medians).

However, the analysis is hampered by covariate imbalance between the IDC and ILC subtypes, as seen in Table 1. More broadly, covariate balance is vitally important in observational studies where interest focuses on unconfounded descriptive comparisons of group potential outcomes (Robins & Rotnitzky 1995, Rubin 2007). Theoretical and simulation studies have demonstrated the conceptual and practical advantages of weighting over other covariate-balancing techniques like matching and regression adjustment (Austin 2010). As a result, weighting methods have widespread applicability in diverse research areas such as political science, sociology, and healthcare (Lunceford & Davidian 2004). For analyzing retrospective cohorts consisting of two groups, the propensity score (PS), or the probability that a subject with given covariates belongs to the reference group (Rosenbaum & Rubin 1983), plays a central role, and the average treatment effect (ATE) and average treatment effect on the treated group (ATT) are overwhelmingly popular estimands (Robins et al. 2000). However, the inverse probability weights (IPW) on which the estimators typically rely are unstable when some PSs are near 0 or 1 (Li & Li 2019).

Several researchers have proposed variations of ATE based on truncated subpopulations of scientific or statistical interest (Crump et al. 2006, Li & Greene 2013). Li et al. (2018) introduced *overlap weights* which, unlike IPWs, are bounded, and under appropriate theoretical conditions, minimize the asymptotic variance of the weighted average treatment effect to estimate the average treatment effect for the overlap population (ATO). Li et al. (2018) also demonstrated that most weighting methods, either implicitly or explicitly, make inferences about predetermined target populations. For single observational studies comprising two or more groups, Li & Li (2019) introduced *generalized overlap weights* that minimize the asymptotic sum of variances of weighted estimators of pairwise group differences. For multiple observational studies with two groups, Wang & Rosner (2019) developed a PS-based integrative approach for Bayesian posterior inferences on ATE.

Table 1: Summary of some demographic, clinicopathological, and biomarker variables of the TCGA breast cancer studies. Shown in parentheses are percentages. **IGC**: International Genomics Consortium; **MSKCC**: Memorial Sloan Kettering Cancer Center; **Pittsburgh**: University of Pittsburgh; **Miami**: University of Miami.

	Walter Reed	IGC	MSKCC	Mayo Clinic	Pittsburgh	Roswell Park	Miami
TOTAL	92	38	35	57	117	81	30
Mean age at diagnosis	56.6	66.4	52.5	54.6	56.7	57.1	57.8
Race							
Asian	2 (2.2)	1 (2.6)	2 (5.7)	1 (1.8)	1 (0.9)	0 (0.0)	1 (3.3)
Black	23 (25.0)	12 (31.6)	5 (14.3)	1 (1.8)	9 (7.7)	14 (17.3)	7 (23.3)
White	67 (72.8)	25 (65.8)	28 (80.0)	55 (96.5)	107 (91.5)	67 (82.7)	22 (73.3)
Cancer in nearby lymph nodes	45 (48.9)	26 (68.4)	18 (51.4)	30 (52.6)	65 (55.6)	42 (51.9)	18 (60.0)
Mean percentage genome altered	28.9	19.4	32.5	30.6	25.8	28.2	29.9
Median year of diagnosis	2008	2011	2006	2006	2008	2009	2010
Menopause status type							
Type 1 or 2	2 (2.2)	3 (7.9)	1 (2.9)	2 (3.5)	9 (7.7)	2 (2.5)	0 (0.0)
Type 3	62 (67.4)	23 (60.5)	19 (54.3)	33 (57.9)	58 (49.6)	54 (66.7)	23 (76.7)
Type 4	28 (30.4)	0 (0.0)	15 (42.9)	22 (38.6)	25 (21.4)	25 (30.9)	4 (13.3)
Type 5	0 (0.0)	12 (31.6)	0 (0.0)	0 (0.0)	25 (21.4)	0 (0.0)	3 (10.0)
Cancer stage							
Stage I	18 (19.6)	2 (5.3)	4 (11.4)	11 (19.3)	37 (31.6)	21 (25.9)	4 (13.3)
Stage II	50 (54.3)	26 (68.4)	24 (68.6)	30 (52.6)	57 (48.7)	45 (55.6)	19 (63.3)
Stage III	20 (21.7)	10 (26.3)	7 (20.0)	16 (28.1)	22 (18.8)	15 (18.5)	7 (23.3)
Stage IV	4 (4.3)	0 (0.0)	0 (0.0)	0 (0.0)	1 (0.9)	0 (0.0)	0 (0.0)
Positive ER status	68 (73.9)	35 (92.1)	25 (71.4)	48 (84.2)	99 (84.6)	60 (74.1)	21 (70.0)
Positive PR status	55 (59.8)	27 (71.1)	24 (68.6)	37 (64.9)	88 (75.2)	55 (67.9)	18 (60.0)
Cancer type							
Infiltrating Ductal Carcinoma (IDC)	72 (78.3)	11 (28.9)	29 (82.9)	40 (70.2)	105 (89.7)	67 (82.7)	23 (76.7)
Infiltrating Lobular Carcinoma (ILC)	20 (21.7)	27 (71.1)	6 (17.1)	17 (29.8)	12 (10.3)	14 (17.3)	7 (23.3)
Mean mRNA expression of gene							
COL9A3	-0.07	0.22	0.00	-0.12	-0.14	0.00	0.27
CXCL12	0.01	0.37	-0.01	0.26	0.34	-0.07	-0.05
IGF1	0.23	0.52	0.14	0.41	0.34	-0.11	0.09
ITGA11	-0.11	-0.22	-0.37	-0.11	0.20	-0.07	-0.11
IVL	-0.30	-0.41	-0.30	-0.43	-0.41	-0.50	-0.42
LEF1	-0.03	0.12	0.09	0.15	0.12	-0.04	0.07
PRB2	-0.85	-0.93	-0.93	-0.82	-0.87	-0.60	-0.78
SMR3B	-0.47	-0.13	-0.57	-0.53	-0.51	-0.64	-0.61

There is a critical need for statistical approaches for integrating multiple observational studies and multiple unbalanced groups. To be broadly applicable and effectual, these techniques must account for between-study heterogeneities and accommodate a wide range of estimands as well as univariate or multivariate outcomes. At least in theory, the aforementioned weighting approaches could be applied by labeling the study-group combinations as "treatments," but this strategy has several problems. First, these methods are guaranteed to be successful for a specific set of outcome types and estimands under certain theoretical conditions (e.g., equal variances of univariate group-specific outcomes). Second, these methods may imply group assignment changes for some subjects that are sometimes difficult to justify for a meaningful, generalizable population (Li et al. 2018, Li & Li 2019). More generally, the previously mentioned weighting approaches may not (i) efficiently analyze multiple observational studies comprising multiple groups, (ii) provide scientifically relevant inferences because their predetermined target populations may differ from the natural population of interest, and (iii) deliver precise inferences for wide-ranging estimands and outcome types.

To overcome these challenges, Guha et al. (2022) introduced *concordant* weights capable of incorporating researcher-specified characteristics of the larger population of interest and achieving covariate balance in multigroup-multistudy settings. This outcome- and estimand-agnostic technique maximizes the effective sample size (ESS) to deliver meaningful inferences for the larger population. Compared to some existing weighting methods, the strategy was found to be precise for meta-analyzing right-censored outcomes and estimating group-specific estimands of censored survival times.

Although the concordant weighting methodology of Guha et al. (2022) opened up new avenues for meta-analysis, important methodological gaps remain. For example, study endpoints that are fully observed (i.e., uncensored) can be continuous, categorical, or multivariate, and inference procedures for disparate outcome types have been inadequately ex-

plored in the literature. Further, scientific interests may necessitate alternative estimands than ATE, ATT or ATO (e.g., distribution percentiles, standard deviations, and pairwise correlations of multivariate outcomes) in addition to unplanned estimands suggested during post hoc analyses. To our knowledge, there are no unified approaches for meta-analyzing various outcome types in multiple observational studies with multiple groups capable of inferences about a broad swath of planned or unplanned estimands.

To bridge these gaps, this paper fosters integrative approaches for unconfounded inferences on a wide variety of population-level group features and estimands relevant to group comparisons. The new weighted estimators are appropriate for quantitative, categorical, and multivariate outcomes. The proposed estimators facilitate the derivation of asymptotic variances under mild theoretical assumptions and can be flexibly applied to estimate various functionals of the group-specific potential outcomes such as contrasts and ratios of means, medians, and standard deviations, in addition to CDFs and distribution percentiles. For undersampled groups for which asymptotic results do not hold, we devise accurate small-sample procedures for quantifying estimation uncertainty. A meta-analysis of the motivating TCGA database shed light on the differential mRNA expression patterns of eight breast cancer genes for the IDC and ILC disease subtypes. Although the different weighting methods made somewhat comparable inferences, the concordant target population produced the narrowest confidence intervals for most of the estimands, and its distinctive findings are supported by recent literature. Comparing the mRNA expression of the targeted genes in the two breast cancer subtypes, the concordant weighting strategy found the average expression levels of the genes CXCL12, IGF1, LEF1, PRB2, and SMR3B, and the expression standard deviation of the genes PRB2, COL9A3 and IVL to be significantly different. Additionally, the differential correlation pattern comprised eight pairs of the targeted genes.

The rest of the paper is organized as follows. Section 2 develops unconfounded in-

tegrative procedures for different weighting methods and various types of estimands and establishes theoretical guarantees under mild conditions. The simulation study of Section 3 illustrates the reliability of the proposed methodology, especially when used in conjunction with concordant weights. Section 4 applies the proposed techniques to meta-analyze the motivating TCGA breast cancer studies, detecting differential biomarker patterns in the two major breast cancer subtypes in the United States and comparing the concordant weights to other weighting methods. Section 5 concludes with some final remarks.

2 Meta-analyzing Potential Outcomes of Multiple Groups

2.1 Notation and brief review of some basic concepts

Consider an investigation in which there are J observational studies with the participants in each study partitioned into K groups determined by an attribute such as sex, race, histology or disease subtype. Let Z_i denote the group and S_i denote the observational study to which subject i belongs, $i = 1 \ldots, N$. Then *bifactor* $\mathbf{\Phi}_i = (S_i, Z_i)$ represents the study-group combination with bifactor values, $\boldsymbol{\varphi} = (s, z)$, belonging to the set Ω consisting of JK pairs. Additionally, there are p covariates denoted by $\mathbf{X}_i$ belonging to $\mathcal{X} \subset \mathcal{R}^p$. For example, the TCGA breast cancer data has $J = 7$ studies, $K = 2$ disease subtypes as the groups, and $p = 30$ covariates on $N = 450$ breast cancer patients. Let N_{sz} be the number of subjects belonging to group z and study s, $N_s = \sum_{z=1}^{K} N_{sz}$ be the number of subjects in study s, and $N_z = \sum_{s=1}^{J} N_{sz}$ be the number of subjects in group z. For $z = 1, \ldots, K$, the zth group's potential outcome of the ith subject is a vector of length L denoted by $\mathbf{Y}_i^{(z)} = (Y_{i1}^{(z)}, \ldots, Y_{iL}^{(z)})'$; thus, the realized or observed outcome is $\mathbf{Y}_i = \mathbf{Y}_i^{(Z_i)}$. For the motivating TCGA data, vectors $\mathbf{Y}_i^{(1)}$ and $\mathbf{Y}_i^{(2)}$ respectively represent the ith patient's *potential* mRNA measurements for disease subtypes IDC and ILC on the $L = 8$ genes. Naturally, observed outcome $\mathbf{Y}_i = \mathbf{Y}_i^{(Z_i)}$ because Z_i represents the disease subtype with

which patient i is actually diagnosed.

If the subject indexes are not meaningful, the data can be regarded as a random sample from a *source density* $[\boldsymbol{\Phi}, \mathbf{X}, \mathbf{Y}]$, where $[\cdot]$ symbolizes densities under appropriate dominating measures. Naive group comparisons are biased because the study memberships, group memberships, and covariates are unbalanced in the source population. In multigroup-multistudy settings, Guha et al. (2022) extended propensity scores to define the bifactor PS (BPS): $e_{\boldsymbol{\varphi}}(\mathbf{x}) = e_{sz}(\mathbf{x}) = P\big(\boldsymbol{\Phi} = \boldsymbol{\varphi} \mid \mathbf{X} = \mathbf{x}\big)$, for $\boldsymbol{\varphi} \in \Omega$ and $\mathbf{x} \in \mathcal{X}$. Although unknown for observational studies, the BPS can be estimated straightforwardly.

Extending Rubin (2007) and Imbens (2000), we make the following basic assumptions. (A) *Stable unit treatment value*: given a subject's covariates, their study and group memberships do not influence the potential outcomes of any other subject; (B) *Weak unconfoundedness*: for each study s, given covariate $\mathbf{X} = \mathbf{x}$, membership in the zth group is independent of the potential outcome $\mathbf{Y}^{(z)}$; and (C) *Positivity*: for each s, the study-specific group PS, $e_{z|s}(\mathbf{x}) = e_{sz}(\mathbf{x}) / \sum_{z'=1}^{K} e_{sz'}(\mathbf{x})$, is strictly positive and less than 1. Assumption (B) states that $[\mathbf{Y}^{(z)} \mid S = s,\, Z = z,\, \mathbf{X} = \mathbf{x}] = [\mathbf{Y}^{(z)} \mid S = s,\, \mathbf{X} = \mathbf{x}]$. Assumption (C) ensures that a subject's group memberships are not deterministic functions of their covariates.

Guha et al. (2022) designed a family of target populations with attributes prescribed by the investigator via two fully or partially probability vectors: (i) relative study weights, $\boldsymbol{\alpha} = (\alpha_1, \ldots, \alpha_J)$; and (ii) relative group prevalence, $\boldsymbol{\beta} = (\beta_1, \ldots, \beta_K)$. For instance, in the TCGA breast cancer studies, setting $\alpha_j = 1/7$ extracts equal amounts of information from each study, whereas $\boldsymbol{\beta} = (8/9, 1/9)$ constrains the target population to the relative proportions of disease in the U.S.A. (Wright 2022, Tran 2022). The relative mass of bifactor $\boldsymbol{\varphi} \in \Omega$ in the target population is then $\delta_{\boldsymbol{\varphi}} = \alpha_s \beta_z$, so that $\sum_{\boldsymbol{\varphi} \in \Omega} \delta_{\boldsymbol{\varphi}} = 1$. If some or all components of $\boldsymbol{\alpha}$ or $\boldsymbol{\beta}$ are unknown, subsequent inferences optimize over the multiple possibilities for $\boldsymbol{\delta} = \{\delta_{\boldsymbol{\varphi}}\}_{\Omega}$.

Let the marginal covariate densities in the source and target populations be denoted by

$f(\mathbf{x})$ and $f^*(\mathbf{x})$ respectively. It can be shown that there exists a *tilting function* λ such that $f^*(\mathbf{x}) = \lambda(\mathbf{x})f(\mathbf{x})/\mathbb{E}[\lambda(\mathbf{X})]$ for all $\mathbf{x} \in \mathcal{X}$, where $\mathbb{E}[\cdot]$ denotes expectations with respect to the source. Informally, high values of the tilting function identify covariate space regions with high relative weight in the target population. Let $[\cdot]_*$ with subscript "$*$" represent densities of the target population and $P_*[\cdot]$ represent target population probabilities. To achieve theoretical covariate balance between the K groups, and because $\boldsymbol{\alpha}$ is closely related to the study designs rather than a realistic natural population, Guha et al. (2022) formulated a family of balanced target populations in which S, Z, and $\mathbf{X}$ are mutually independent, i.e., for $\boldsymbol{\varphi} \in \Omega$ and $\mathbf{x} \in \mathcal{X}$,

$$\big[\boldsymbol{\Phi} = \boldsymbol{\varphi}, \mathbf{X} = \mathbf{x}\big]_* = \alpha_s \, \beta_z \, f^*(\mathbf{x}) = \frac{\delta_{\boldsymbol{\varphi}} \lambda(\mathbf{x}) f(\mathbf{x})}{\mathbb{E}[\lambda(\mathbf{X})]}. \tag{1}$$

Thus, $P_*[\boldsymbol{\Phi} = \boldsymbol{\varphi}] = \delta_{\boldsymbol{\varphi}}$ for the target population, providing the investigator control over key population features through the full or partial specification of $\boldsymbol{\alpha}$ and $\boldsymbol{\beta}$. Source density $f(\mathbf{x})$ is invariant; hence, each $(\boldsymbol{\delta}, \lambda)$ consistent with researcher input gives an *admissible* target population in (1). Guha et al. (2022) associated a set of *generalized balancing weights* that apportion realizations from the source population so that they are distributed as the target population: $w_{\boldsymbol{\varphi}}(\mathbf{x}) = \big[\boldsymbol{\Phi} = \boldsymbol{\varphi}, \mathbf{X} = \mathbf{x}\big]_* / \big[\boldsymbol{\Phi} = \boldsymbol{\varphi}, \mathbf{X} = \mathbf{x}\big] = \frac{\delta_{\boldsymbol{\varphi}} \lambda(\mathbf{x})}{e_{\boldsymbol{\varphi}}(\mathbf{x}) \mathbb{E}[\lambda(\mathbf{X})]}$. Defining $\tilde{w}_{\boldsymbol{\varphi}}(\mathbf{x}) = \delta_{\boldsymbol{\varphi}} \lambda(\mathbf{x}) / e_{\boldsymbol{\varphi}}(\mathbf{x})$, the empirically normalized weights, $\bar{w}_i = N \tilde{w}_{\boldsymbol{\varphi}_i}(\mathbf{x}_i) / \sum_{l=1}^{N} \tilde{w}_{\boldsymbol{\varphi}_l(\mathbf{x}_l)}$, have sample average 1 and do not depend on normalizing constant $\mathbb{E}[\lambda(\mathbf{X})]$. Guha et al. (2022) showed that the normalized weights achieve *sample* covariate balance as N grows. Table 2 of Guha et al. (2022) demonstrates how several existing weighting strategies in the literature can be extended to multistudy-multigroup settings using specification (1). Specifically, inverse probability weights and overlap weights are generalized to the *combined* and MGO target populations, respectively.

Concordant target population Different target populations identified by $\boldsymbol{\delta}$ and λ can be evaluated using the *effective sample size* (ESS), $\mathcal{E}(\boldsymbol{\delta}, \lambda) = N/\big[1 + \text{Var}\big\{w_{\boldsymbol{\Phi}}(\mathbf{X})\big\}\big] = N/\mathbb{E}\big[w^2_{\boldsymbol{\Phi}}(\mathbf{X})\big]$, provided the generalized balancing weights have a finite second moment under the source. The sample ESS, $\hat{\mathcal{E}}(\boldsymbol{\delta}, \lambda) = N^2/\sum_{i=1}^{n} \bar{w}_i^2$, is a consistent estimator. Informally, the ESS represents the hypothetical sample size from the target population that achieves the same inferential precision as sample size N from the source. The *concordant population* is defined as the admissible target population that maximizes ESS. That is, $\mathcal{E}(\breve{\boldsymbol{\delta}}, \breve{\lambda}) = \max_{\boldsymbol{\delta},\lambda} \mathcal{E}(\boldsymbol{\delta}, \lambda)$ subject to the fully or partially specified $\boldsymbol{\alpha}$ and $\boldsymbol{\beta}$. Guha et al. (2022) showed that the global supremum of the concordant tilting function $\breve{\lambda}$ over the covariate space is 1. Under appropriate conditions, the supremum is attained at covariate vectors for which the bifactor PS equals the bifactor relative mass for every study-group combination. Informally, the concordant population upweights covariate regions where the group propensities of the sample match the group proportions of the natural population.

The strategy of Guha et al. (2022) provides opportunities for integrating observational studies to analyze right-censored outcomes and estimating different estimands related to survival times. However, there is limited guidance in the literature about weighting procedures for fully observed continuous, categorical, or multivariate outcomes, especially in multistudy-multigroup investigations that prioritize estimands besides ATE, ATT, and ATO. In addition to providing general inferential approaches for existing weighting methods, the present work demonstrates the high accuracies achieved by the "outcome-free" concordant weights that disregard specific estimands, estimators, and study endpoints.

2.2 Inferences of potential group outcomes with fully observed endpoints

For a target population with structure (1), which as mentioned encompasses several weighting methods including the concordant target poulation, we present new unconfounded inference strategies for various population-level features of the study endpoints. Suppose the potential outcomes $\mathbf{Y}^{(1)}, \ldots, \mathbf{Y}^{(K)} \in \mathcal{R}^L$ have a common support, $\mathcal{Y}$. We assume that the outcome distribution given random vector $\mathbf{\Phi}$ is identical in the source and target: for each bifactor $\boldsymbol{\varphi} = (s, z) \in \Omega$ and covariate $\mathbf{x} \in \mathcal{X}$,

$$[\mathbf{Y} \mid S = s, Z = z, \mathbf{X} = \mathbf{x}]_* = [\mathbf{Y} \mid S = s, Z = z, \mathbf{X} = \mathbf{x}], \tag{2}$$

where, as before, $[\cdot]$ with (without) the subscript "$*$" denotes densities in the target (source) population. As in the source population, weak unconfoundedness gives us

$$[\mathbf{Y}|\mathbf{\Phi} = \boldsymbol{\varphi}, \mathbf{X} = \mathbf{x}]_* = [\mathbf{Y}^{(z)}|S = s, \mathbf{X} = \mathbf{x}]_*$$

independently of group membership. However, unlike the source population,

$$[\mathbf{Y} \mid Z = z]_* = [\mathbf{Y}^{(z)}]_* \tag{3}$$

for the covariate-balanced target. We make use of this important property to construct weighted estimators of target population features.

As before, let $\mathbb{E}[\cdot]$ and $\mathbb{E}[\cdot]_*$ denote expectations with respect to the source and target populations, respectively. Let $h_1, \ldots, h_M$ be real-valued functions with domain $\mathcal{Y}$. Suppose we wish to infer target population means of the transformed potential outcomes, $\mathbb{E}[h_1(\mathbf{Y}^{(z)})]_*, \ldots, \mathbb{E}[h_M(\mathbf{Y}^{(z)})]_*$ for group $z = 1, \ldots, K$. Appropriate choices of h_m corre-

spond to target population inferences about marginal means, medians, and variances, as well as marginal CDFs of group-specific potential outcome components. Equivalently, the primary inferential focus is

$$\boldsymbol{\mu}^{(z)} = \mathbb{E}[\boldsymbol{h}(\mathbf{Y}^{(z)})]_* \quad \text{where, for } \mathbf{y} \in \mathcal{Y} \subset \mathcal{R}^L,$$
$$\boldsymbol{h}(\mathbf{y}) = \begin{pmatrix} h_1(\mathbf{y}) \\ \vdots \\ h_M(\mathbf{y}) \end{pmatrix} \in \mathcal{R}^M.$$

For real-valued functions π with domain $\mathcal{R}^M$, we are also interested in estimating $\pi(\boldsymbol{\mu}^{(z)})$. For example, if the first two components of $\mathbf{Y}^{(z)}$ are quantitative, then with $h_1(\mathbf{Y}^{(z)}) = Y_1^{(z)}$, $h_2(\mathbf{Y}^{(z)}) = Y_2^{(z)}$, $h_3(\mathbf{Y}^{(z)}) = Y_1^{(z)}Y_2^{(z)}$, and defining $\pi(t_1, t_2, t_3) = t_3 - t_1 t_2$, we obtain $\pi(\boldsymbol{\mu}^{(z)}) = \text{cov}(Y_1^{(z)}, Y_2^{(z)})_*$ as the target population covariance. The target population correlation of pairwise components of $\mathbf{Y}^{(z)}$ can be estimated from estimates of the covariance and standard deviations. In the TCGA study, it is of interest to estimate the correlations among the eight targeted genes for groups $z = 1, 2$ (i.e., IDC and ILC subtypes).

For a general weighting method, utilizing the empirically normalized balancing weights, we propose estimating $\mathbb{E}[\boldsymbol{h}(\mathbf{Y}^{(z)})]_*$ as

$$\bar{\boldsymbol{h}}_z = \frac{1}{N\beta_z} \sum_{i=1}^{N} \bar{w}_i \, \boldsymbol{h}(\mathbf{Y}_i) \, \mathcal{I}(Z_i = z). \tag{4}$$

Estimator (4) has several noteworthy features: (i) as shown in Theorem 2.1 below, the estimator is consistent and asymptotically multivariate normal as N grows; (ii) it is applicable to any set of balancing weights and their target populations, including combined, MGO, and concordant weights; (iii) it generalizes weighted estimators of average controlled difference (ACD) (Hirano & Imbens 2001, Li et al. 2018) and plug-in sample moment estimators (Li & Li 2019) to multiple groups and studies, while accommodating a much broader class of

potential outcomes (e.g., multivariate outcomes), and (iv) it exploits known or researcher-supplied information about the group proportions of the target population; as previously mentioned, the concordant weights typically assign β_z to match known group prevalences of the larger population. By contrast, $\beta_z = 1/K$ for most other weighting methods.

The following theorem and corollaries study asymptotic properties of random vector $\bar{\boldsymbol{h}}_z$ as an estimator of the multivariate feature $\mathbb{E}[\boldsymbol{h}(\mathbf{Y}^{(z)})]_*$. The proofs are available in the Appendix.

Theorem 2.1. *Let $\mathbb{E}[\cdot]$ and $\mathbb{E}[\cdot]_*$ denote expectations with respect to the source and target populations, respectively. Let source probability $P[S = s]$ be strictly positive for study $s = 1, \ldots, J$. Suppose the conditional distributions of the potential outcomes are weakly unconfounded, as described in Section 2.1, and satisfy assumption (2). For a target population of the form (1), let the random balancing weights be such that $\mathbb{E}[w^2_{\boldsymbol{\Phi}}(\mathbf{X})]$ is finite.*

For $m = 1, \ldots, M$, suppose h_m is a real-valued function with domain $\mathcal{Y}$ for which the source population moment $\mathbb{E}[w_{\boldsymbol{\Phi}}(\mathbf{X})h_m(\mathbf{Y})]$ is finite. Interest focuses on target population moment $\mathbb{E}[\boldsymbol{h}(\mathbf{Y}^{(z)})]_*$ which is also written as vector $\boldsymbol{\mu}^{(z)} = (\mu_1^{(z)}, \ldots, \mu_M^{(z)})'$. Then estimator $\bar{\boldsymbol{h}}_z$ defined in (4) has the following properties as $N \to \infty$:

1. ***Consistency**: $\bar{\boldsymbol{h}}_z \xrightarrow{p} \boldsymbol{\mu}^{(z)}$.*

2. ***Asymptotic normality**: For $m = 1, \ldots, M$, suppose source moment $\mathbb{E}[w^2_{\boldsymbol{\Phi}}(\mathbf{X})h^2_m(\mathbf{Y})]$ is finite. Then*

$$\sqrt{N}\left(\bar{\boldsymbol{h}}_z - \boldsymbol{\mu}^{(z)}\right) \xrightarrow{d} N_M\big(\mathbf{0}, \boldsymbol{\Sigma}^{(z)}\big), \tag{5}$$

where matrix $\boldsymbol{\Sigma}^{(z)}$ consists of the elements

$$\big(\sigma^{(z)}_{mm'}\big)^2 = \frac{1}{\beta_z^2}\mathbb{E}\left[w^2_{\boldsymbol{\Phi}}(\mathbf{X})\left(h_m(\mathbf{Y})\,\mathcal{I}(Z = z) - \beta_z\mu_m^{(z)}\right)\left(h_{m'}(\mathbf{Y})\,\mathcal{I}(Z = z) - \beta_z\mu_{m'}^{(z)}\right)\right], \tag{6}$$

for $m, m' = 1, \ldots, M$.

3. A consistent estimator of matrix $\boldsymbol{\Sigma}^{(z)}$ *is* $\hat{\boldsymbol{\Sigma}}^{(z)}$ *with typical element*

$$\big(s^{(z)}_{mm'}\big)^2 = \frac{1}{N\beta_z^2}\sum_{i=1}^{N}\bar{w}_i^2\Big(h_m(\mathbf{Y}_i)\,\mathcal{I}(Z_i=z)-\beta_z\bar{h}_{zm}\Big)\Big(h_{m'}(\mathbf{Y}_i)\,\mathcal{I}(Z_i=z)-\beta_z\bar{h}_{zm'}\Big),$$

for $m, m' = 1, \ldots, M$*, where the* m*th component of vector* $\bar{\boldsymbol{h}}_z$ *is denoted by* $\bar{h}_{zm}$*. If* $\boldsymbol{\Sigma}^{(z)}$ *is invertible, then*

$$\sqrt{N}\hat{\mathbf{A}}_z\Big(\bar{\boldsymbol{h}}_z-\boldsymbol{\mu}^{(z)}\Big)\xrightarrow{d} N_M\big(\mathbf{0},\mathbf{I}\big),$$

where $\hat{\mathbf{A}}_z = \big(\hat{\boldsymbol{\Sigma}}^{(z)}\big)^{-1/2}$.

Corollary 2.1.1. *For the* ***concordant target population****, the sufficient conditions are considerably simplified if the study weights* α_s *are all strictly positive. Assume that source probability* $P[S=s]$ *of each study is positive, and that the potential outcomes are conditionally weakly unconfounded and satisfy assumption (2). Then Parts 1-3 of Theorem 2.1 hold provided source moment* $\mathbb{E}[h_m^2(\mathbf{Y})]$ *exists for all* $m = 1, \ldots, M$.

The next result investigates asymptotic properties of an estimator of $\pi(\boldsymbol{\mu}^{(z)})$:

Corollary 2.1.2. *Consider a target population of the form (1). Let* π *be a real-valued differentiable function with domain* $\mathcal{R}^M$*. Let* $\nabla\pi(\boldsymbol{\mu}) = \partial\pi(\boldsymbol{\mu})/\partial\boldsymbol{\mu}$ *denote the gradient vector of length* M *at* $\boldsymbol{\mu}$*. With matrix* $\boldsymbol{\Sigma}^{(z)}$ *defined in (6), suppose the scalar* $\nabla'\pi(\boldsymbol{\mu}^{(z)})\,\boldsymbol{\Sigma}^{(z)}\,\nabla\pi(\boldsymbol{\mu}^{(z)})$ *is positive at* $\boldsymbol{\mu}^{(z)} = \mathbb{E}[\boldsymbol{h}(\mathbf{Y}^{(z)})]_*$*. Define* $\hat{\tau}_z = \nabla'\pi(\bar{\boldsymbol{h}}_z)\,\hat{\boldsymbol{\Sigma}}^{(z)}\,\nabla\pi(\bar{\boldsymbol{h}}_z)$ *if the right hand quantity is positive; otherwise, let* $\hat{\tau}_z$ *be an arbitrary number. Then* $\pi(\bar{\boldsymbol{h}}_z)$ *is a consistent and asymptotically normal estimator of* $\pi(\boldsymbol{\mu}^{(z)})$*:*

$$\frac{\sqrt{N}}{\hat{\tau}_z}\Big(\pi(\bar{\boldsymbol{h}}_z)-\pi(\boldsymbol{\mu}^{(z)})\Big)\xrightarrow{d} N\big(0,1\big).$$

Group comparisons

The multivariate estimators $\bar{\boldsymbol{h}}_1, \ldots, \bar{\boldsymbol{h}}_K$ are mutually independent when the study, group, and covariates of the N subjects are known. For each group z, consider the moment $\mathbb{E}[h_m(\mathbf{Y}^{(z)})]_*$ with estimate $\bar{h}_{zm}$. Applying standard results (e.g., Johnson et al. 2002, Chapter 5), we can make approximate $100(1-\alpha)\%$ confidence statements *simultaneously* for all possible linear combinations of $\mathbb{E}[h_m(\mathbf{Y}^{(1)})]_*, \ldots, \mathbb{E}[h_m(\mathbf{Y}^{(K)})]_*$. If N is large, using the mth diagonal element of $\hat{\boldsymbol{\Sigma}}^{(z)}$ defined in Part 3 of Theorem 2.1, the interval $\sum_{z=1}^K a_z \bar{h}_{zm} \pm s_{mm}^{(z)} \sqrt{\chi^2_K(\alpha) \sum_{z=1}^K a_z^2 \hat{\sigma}^2_{hz}/N}$ will contain $\sum_{z=1}^K a_z \mathbb{E}[h_m(\mathbf{Y}^{(z)})]_*$ with approximate probability $(1-\alpha)$ simultaneously for all possible scalars $a_1, \ldots, a_K$.

A variety of target population features can then be estimated for the K groups. Writing $\mu^{(zm)} = \mathbb{E}[h_m(\mathbf{Y}^{(z)})]_*$, we could estimate contrasts such as $\mu^{(1m)} - \mu^{(2m)}$ (e.g., average difference between the mth gene's mRNA expression levels for IDC and ILC breast cancer patients) and, when $K > 2$, $\mu^{(1m)} - \frac{1}{K-1}\sum_{z=2}^K \mu^{(zm)}$ (e.g., for the mth gene, average difference between the mRNA expression levels for a reference group and the average of the other groups). We can also estimate ratios of means such as $\mu^{(zm)}/\mu^{(1m)}$, ratios of mean differences such as $\left(\mu^{(3m)} - \mu^{(1m)}\right)/\left(\mu^{(2m)} - \mu^{(1m)}\right)$, group-specific standard deviations, percentiles, ratios of medians, and ratios of coefficients of variation. Under mild conditions, many of these estimators are consistent and asymptotically normal, and their asymptotic variances could be derived by applying Corollary 2.1.2 and the delta method.

Uncertainty estimation for small sample sizes or rare groups

Consider a real-valued target population feature of interest generically denoted by θ. In many instances, Theorem 2.1 or its corollaries provide an estimator $\hat{\theta}$ for a suitable choice of functions $\boldsymbol{h}$ and π. However, if sample size N_z is small for some groups, such as undersampled racial minorities, then the asymptotic confidence intervals for θ may have very

different coverage than the nominal levels. We may then employ nonparametric bootstrap methods (Efron & Tibshirani 1994, Singh 1981, Bickel & Freedman 1981, Van der Vaart 2000) to estimate the standard error τ_θ of estimator $\hat{\theta}$ as follows.

For patient $i = 1, \ldots, N$, let $\boldsymbol{\xi}_i = (\boldsymbol{\varphi}_i, \mathbf{x}_i, y_i)$. Using the empirically normalized concordant weights, we draw B bootstrap samples of size N from the mixture distribution, $F^* = \frac{1}{N}\sum_{i=1}^{N} \zeta_{\boldsymbol{\xi}_i}$, where $\zeta_{\boldsymbol{\xi}}$ represents a point mass at $\boldsymbol{\xi}$. Denote by $\boldsymbol{\xi}_i^{(b)}$ the tth draw in the bth bootstrap sample, so that $\boldsymbol{\xi}_t^{(b)} \overset{iid}{\sim} F^*$. Let $\hat{\theta}^{(b)}$ be the concordant-weighted estimate of feature θ based on the bth bootstrap sample. Then a bootstrap estimate of standard error τ_θ is

$$\hat{\tau}_\theta = \left\{ \frac{1}{B-1} \sum_{b=1}^{B} \left(\hat{\theta}^{(b)} - \bar{\theta} \right)^2 \right\}^{1/2},$$

where $\bar{\theta} = \sum_{b=1}^{B} \hat{\theta}^{(b)}/B$. For a fixed sample size N, we have $\hat{\tau}_\theta \xrightarrow{p} \tau_\theta$ as $B \to \infty$. For large B, $\hat{\tau}_\theta$ can be used to construct 95% confidence intervals for θ. Alternatively, the 2.5th and 97.5th percentiles of $\hat{\theta}^{(1)}, \ldots, \hat{\theta}^{(B)}$ give distribution-free 95% confidence intervals for the target population feature θ.

3 Simulation Study

We analyzed 100 artificial databases, each comprised of $J = 4$ retrospective patient cohorts, $K = 3$ racial categories as the groups, and $N = 10,000$ patients. The $N = 10,000$ covariate vectors of length $p = 13$ were randomly sampled without replacement from a publicly available TCGA dataset consisting of 340 glioblastoma multiforme patients. Since the artificial patient-specific outcomes are univariate in this example (i.e., $L = 1$), we simplify the notation by suppressing subscript l throughout. We considered two similarity scenarios of the patient characteristics between the $JK = 12$ study-group combinations. Each covariate had a zero, linear, or quadratic relationship with the study-group memberships of the patients, characterized by the BPS. We assumed a similar set of possible relationships

for the patient outcomes and each covariate. The generation procedure was as follows:

1. **Covariates** For $i = 1, \ldots, N = 10,000$, and $p = 13$, randomly sample, without replacement, the vectors $\mathbf{x}_i = (x_{i1}, \ldots, x_{ip})'$ from the set of patient characteristics in the TCGA glioblastoma multiforme dataset.

2. **Study-group memberships in two similarity scenarios** The study s_i and group z_i of patients $i = 1, \ldots, N$, were generated by the following sequence of steps:

   (a) *Non-predictor, linear or quadratic covariate predictors:* Independently for $t = 1, \ldots, p$, generate categorical variable χ_t with $P[\chi_t = 0] = 0.5$, $P[\chi_t = 1] = 0.25$, and $P[\chi_t = 2] = 0.25$. The three categories of χ_t correspond to the tth covariate being a non-predictor, linear and nonlinear predictor of BPS. The $\Upsilon_1 = \sum_t^p \mathcal{I}(\chi_t > 0)$ number of N-vectors of the linear and quadratic predictors for BPS are arranged in the matrix $\mathbf{Q}_1 = \{x_{it}^{\chi_t} : \chi_t > 0, i = 1, \ldots, N\}$ of dimension $N \times \Upsilon_1$. Let the rows of $\mathbf{Q}_1$ be denoted by $\mathbf{q}_{11}', \ldots, \mathbf{q}_{N1}'$, and define the symmetric positive-definite matrix, $\mathbf{\Gamma}_1 = \left(\mathbf{Q}_1'\mathbf{Q}_1\right)^{-1}$.

   (b) *Similarity scenarios* Suppose *similarity parameter* ω is given. Generate location parameters $\pi_{sz} \overset{\text{i.i.d.}}{\sim} N(0, \omega^2)$ for study $s = 1, \ldots, J$, and group $z = 1, \ldots, K$. Let $(s, z) = (1, 1)$ be the "reference" study-group combination for which the regression coefficient vector is $\boldsymbol{\varsigma}_{11} = \mathbf{0}_{\Upsilon_1}$, a Υ_1-vector of zeros. For the other study-group combinations, independently generate coefficient vector, $\boldsymbol{\varsigma}_{sz} \sim N_{\Upsilon_1}\left(\pi_{sz}\mathbf{1}_{\Upsilon_1}, \mathbf{\Gamma}_1\right)$, where $(s, z) \neq (1, 1)$. Let $\eta_{isz} = \mathbf{q}_{i1}'\boldsymbol{\varsigma}_{sz}$. Compute the BPS as $e_{sz}(\mathbf{x}_i) = \exp(\eta_{isz}) / \sum_{s'=1}^{J} \sum_{z'=1}^{K} \exp(\eta_{is'z'})$.

   We have found that BPS with this structure approaches $1/JK$ for every study-group combination as $\omega \to 0$, and approaches 1 for some study-group combinations as ω grows. Consequently, we considered two scenarios corresponding to "small" and "large" ω: *(i) High similarity*: Setting $\omega = 50\varepsilon$, where ε is the

smallest eigenvalue of matrix $\mathbf{\Gamma}_1$, results in similar covariate distributions for the JK study-group combinations, and *(ii) Low similarity*: Setting $\omega = 100\varepsilon$ produces dissimilar and unbalanced covariate distributions, with propensities near 1 for some study-group combinations and covariate vectors.

(c) *Study-group memberships* For patient $i = 1, \ldots, N$, independently generate (s_i, z_i) from the discrete distribution that assigns probability e_{sz} to study-group combination (s, z) for $s = 1, \ldots, J$ and $z = 1, \ldots, K$.

3. **Patient-specific outcomes** Univariate outcomes $Y_1, \ldots, Y_N$ are generated as follows:

(a) Similarly to the study-group memberships of Step 2, each covariate is allowed to have a zero, linear, or nonlinear association with the outcomes, resulting in a predictor matrix $\mathbf{Q}_2$ of dimension $N \times \Upsilon_2$ with rows $\mathbf{q}'_{12}, \ldots, \mathbf{q}'_{N2}$.

(b) Let $\mathbf{\Gamma}_2 = \sqrt{N}\big(\mathbf{Q}'_2\mathbf{Q}_2\big)^{-1}$. For study $s = 1, \ldots, J$, generate regression vectors $\boldsymbol{\upsilon}_s = (\upsilon_{s1}, \ldots, \upsilon_{s\Upsilon_2})' \overset{\text{i.i.d.}}{\sim} N_{\Upsilon_2}\big(\boldsymbol{\upsilon}_0, \frac{1}{10}\mathbf{\Gamma}_2\big)$, where mean vector $\boldsymbol{\upsilon}_0 \sim N_{\Upsilon_2}\big(\mathbf{0}, \mathbf{\Gamma}_2\big)$.

(c) For patient $i = 1, \ldots, N$, generate $Y_i \overset{\text{indep}}{\sim} N\big(\mathbf{q}'_{12}\boldsymbol{\upsilon}_{s_i}, \tau_2^2\big)$, choosing the error variance so that the multiple R-squared is approximately 0.8.

While analyzing each database, we ignored knowledge of all the simulation parameters, including the predictor covariates and their associations with BPS and the patient outcomes. First, the estimated BPS, $\hat{e}_{\boldsymbol{\varphi}_i}(\mathbf{x}_i)$, for patient $i = 1, \ldots, N$, was obtained using random forests. Using these estimates, we obtained the empirically normalized concordant weights $\bar{w}_1, \ldots, \bar{w}_N$, as outlined in Section 2.1. The computational costs of the calculations were insignificant.

We compared the weighting procedures based on their *percent ESS*, defined as the effective sample size for 100 patients. Summarizing over the 100 independent replications,

	Low similarity			High similarity		
	Concordant	**MGO**	**Combined**	**Concordant**	**MGO**	**Combined**
Minimum	52.43	23.60	23.61	78.07	56.74	56.75
First quartile	72.10	41.44	41.45	87.91	77.70	77.70
Median	78.84	49.18	49.18	91.21	81.86	81.86
Mean	77.39	49.95	49.95	90.37	81.52	81.52
Third quartile	84.12	57.91	57.90	93.54	86.51	86.51
Maximum	96.26	81.17	81.15	97.55	94.75	94.75

Table 2: For the 100 databases of the simulation study, summaries of the percentage ESS of the three target populations in the low and high similarity scenarios.

Table 2 presents the percent ESS of the concordant, MGO, and combined target populations in the two similarity scenarios. As expected, all three weighting methods did better in the high similarity scenario. The combined and MGO target population had comparable ESS in both scenarios, with a median ESS of 49.18% (81.86%) in the low (high) simulation scenarios. By comparison, the concordant target population had a higher median ESS of 78.84% and 91.21%% in the low and high scenarios, respectively. For $N = 10,000$ patients, these percentages correspond to an ESS of 7,884 and 9,121 patients in these scenarios.

Next, we made inferences about various features of the potential outcomes with the three weighting strategies. From a theoretical perspective, it is easily verified that the concordant target population satisfies the sufficient conditions of Corollaries 2.1.1 and 2.1.2 for each potential outcome feature that we investigated. Since the target population features vary with the weighting scheme, we evaluated the accuracy of each estimator with respective to its own target estimand computed by Monte Carlo methods. We considered several potential outcomes features that are functionals of the groups-specific means $\mu^{(z)}$ and standard deviations $\sigma^{(z)}$. The groups-specific medians $M^{(z)}$ were evaluated by first estimating the group-specific CDFs of the potential outcomes.

Tables 3 and 4 display the MSEs and variances for the 100 simulated datasets in the low and high similarity scenarios. We find that in both scenarios, the lowest MSEs and vari-

Low similarity scenario			
MSE			
Estimand	**Concordant**	**MGO**	**Combined**
$\mu^{(1)}$	**862.32**	1,209.48	1,211.39
$\mu^{(2)}$	**519.94**	1,004.13	1,004.00
$\mu^{(3)}$	**1,367.97**	1,825.24	1,826.98
$\sigma^{(1)}$	**11,356.94**	13,641.59	13,672.16
$\sigma^{(2)}$	**9,684.02**	18,658.32	18,666.00
$\sigma^{(3)}$	**10,134.10**	14,302.81	14,308.23
$M^{(1)}$	0.02	0.02	0.02
$M^{(2)}$	0.01	0.01	0.01
$M^{(3)}$	0.03	0.03	0.03
$\mu^{(1)} - \mu^{(2)}$	**1,507.00**	2,604.33	2,606.16
$\mu^{(1)} - \mu^{(3)}$	**2,720.10**	5,064.43	5,071.85
$\mu^{(2)} - \mu^{(3)}$	**2,388.91**	4,447.68	4,448.99
$\mu^{(1)} - \bar{\mu}$	**1,516.32**	2,722.46	2,726.76
$\mu^{(2)} - \bar{\mu}$	**1,267.92**	2,259.90	2,259.61
$\mu^{(3)} - \bar{\mu}$	**2,177.76**	4,104.97	4,108.88
$\mu^{(1)}/\mu^{(2)}$	**0.0016**	0.0027	0.0027
$\mu^{(1)}/\mu^{(3)}$	**0.0032**	0.0059	0.0059
$\mu^{(2)}/\mu^{(3)}$	**0.0028**	0.0051	0.0051
Variance			
Estimand	**Concordant**	**MGO**	**Combined**
$\mu^{(1)}$	**847.59**	1,133.62	1,135.13
$\mu^{(2)}$	**516.51**	1,001.57	1,001.42
$\mu^{(3)}$	**1,278.64**	1,719.78	1,720.91
$\sigma^{(1)}$	**4,288.89**	5,572.66	5,585.89
$\sigma^{(2)}$	**3,498.11**	3,913.94	3,927.47
$\sigma^{(3)}$	**5,057.01**	5,750.76	5,769.72
$M^{(1)}$	0.01	0.01	0.01
$M^{(2)}$	0.01	0.01	0.01
$M^{(3)}$	0.01	0.01	0.01
$\mu^{(1)} - \mu^{(2)}$	**1,474.62**	2,553.77	2,555.37
$\mu^{(1)} - \mu^{(3)}$	**2,543.52**	4,704.20	4,709.64
$\mu^{(2)} - \mu^{(3)}$	**2,331.18**	4,306.81	4,307.27
$\mu^{(1)} - \bar{\mu}$	**1,426.28**	2,552.28	2,555.69
$\mu^{(2)} - \bar{\mu}$	**1,267.01**	2,254.24	2,253.91
$\mu^{(3)} - \bar{\mu}$	**2,068.70**	3,867.06	3,869.62
$\mu^{(1)}/\mu^{(2)}$	**0.0015**	0.0026	0.0026
$\mu^{(1)}/\mu^{(3)}$	**0.0030**	0.0055	0.0055
$\mu^{(2)}/\mu^{(3)}$	**0.0027**	0.0049	0.0049

Table 3: For the **low similarity** scenario of the simulation study, estimated MSEs and variances of potential outcome features in the different target populations. For each feature (row), the best weighting strategy (column) is marked in bold.

High similarity scenario			
MSE			
Estimand	**Concordant**	**MGO**	**Combined**
$\mu^{(1)}$	**220.95**	227.09	226.94
$\mu^{(2)}$	**257.07**	322.30	322.31
$\mu^{(3)}$	**279.77**	324.26	324.42
$\sigma^{(1)}$	4,252.39	**4,104.49**	4,111.44
$\sigma^{(2)}$	**3,331.10**	3,929.71	3,932.85
$\sigma^{(3)}$	2,177.**61**	2,412.82	2,416.67
$M^{(1)}$	0.02	0.02	0.02
$M^{(2)}$	0.01	0.01	0.01
$M^{(3)}$	0.03	0.03	0.03
$\mu^{(1)} - \mu^{(2)}$	**655.20**	774.63	774.19
$\mu^{(1)} - \mu^{(3)}$	**696.73**	779.87	779.90
$\mu^{(2)} - \mu^{(3)}$	**872.85**	1,066.35	1,066.85
$\mu^{(1)} - \bar{\mu}$	**457.76**	510.66	510.33
$\mu^{(2)} - \bar{\mu}$	**589.84**	725.52	725.55
$\mu^{(3)} - \bar{\mu}$	**620.99**	729.45	729.82
$\mu^{(1)}/\mu^{(2)}$	**0.0007**	0.0008	0.0008
$\mu^{(1)}/\mu^{(3)}$	**0.0007**	0.0008	0.0008
$\mu^{(2)}/\mu^{(3)}$	**0.0009**	0.0011	0.0011
Variance			
Estimand	**Concordant**	**MGO**	**Combined**
$\mu^{(1)}$	**217.79**	222.14	221.98
$\mu^{(2)}$	**232.75**	288.15	288.22
$\mu^{(3)}$	**224.57**	259.84	260.02
$\sigma^{(1)}$	**1,720.89**	1,851.01	1,867.88
$\sigma^{(2)}$	1,892.24	1,658.72	**1,657.98**
$\sigma^{(3)}$	1,838.31	**1,813.78**	1,817.93
$M^{(1)}$	0.01	0.01	0.01
$M^{(2)}$	0.01	0.01	0.01
$M^{(3)}$	0.01	0.01	0.01
$\mu^{(1)} - \mu^{(2)}$	**645.24**	761.52	761.15
$\mu^{(1)} - \mu^{(3)}$	**611.99**	674.81	674.79
$\mu^{(2)} - \mu^{(3)}$	**720.04**	873.97	874.64
$\mu^{(1)} - \bar{\mu}$	**448.61**	499.68	499.31
$\mu^{(2)} - \bar{\mu}$	**529.64**	649.04	649.19
$\mu^{(3)} - \bar{\mu}$	**504.71**	584.01	584.43
$\mu^{(1)}/\mu^{(2)}$	**0.0006**	0.0008	0.0008
$\mu^{(1)}/\mu^{(3)}$	**0.0006**	0.0007	0.0007
$\mu^{(2)}/\mu^{(3)}$	**0.0007**	0.0009	0.0009

Table 4: For the **high similarity** scenario of the simulation study, estimated MSEs and variances of potential outcome features in the different target populations. For each feature (row), the best weighting strategy (column) is marked in bold.

ances (marked in bold for each feature) correspond to the concordant target population and that substantial reductions are often achieved relative to the other methods. Surprisingly, this includes the pairwise ATEs for which the MGO weights are optimal under additional theoretical assumptions such as homoscedasticity (see Li & Li 2019, for a justification in the single study situation); however, some of these assumptions are not satisfied by the simulation mechanism of the current investigation. In contrast, finite second moments of the source distribution is the only sufficient condition in Corollaries 2.1.1 and 2.1.2 for a wide variety of outcome features of the concordant target population. The MGO and combined weights had somewhat similar performances for these data. The results demonstrate the theoretical and practical advantages of the concordant strategy that focuses on stabilizing the balancing weights rather than specific estimands such as pairwise ATEs. The benefits of the concordant weights are greater in the more challenging low similarity scenario where the racial groups and covariates are highly imbalanced for the $JK = 12$ study-group combinations.

4 Data Analysis

We meta-analyzed the $J = 7$ motivating TCGA studies to investigate breast cancer oncogenesis using mRNA expression measurements on the $L = 8$ targeted genes. The data involve $n = 450$ breast cancer patients partitioned into $K = 2$ groups determined by cancer subtype (IDC and ILC), and $p = 30$ demographic and clinicopathological covariates for each patient. Although IDC and ILC make up approximately 80% and 10% of all U.S. breast cancer cases (Wright 2022, Tran 2022), the relative proportions are significantly different for each TCGA study in Table 1. Applying the two-step iterative procedure of Guha et al. (2022), the concordant weights facilitate unconfounded inferences for estimands of interest while constraining the target population to the known relative proportions of IDC and ILC

in the U.S.A. By contrast, all the other weighting methods reviewed in Sections 1 and 2.1 assume synthetic target populations with equal proportions of disease subtypes, possibly affecting the validity of their inferences.

The percent ESS of the combined population was 25.7% or 115.7 patients. The MGO population had similar ESS of 26.4% or 118.7 patients. The concordant population achieved a higher percent ESS of 40.9% or 183.9 patients, in addition to ensuring that the weighted proportion of IDC and ILC patients in each TCGA study matched that of U.S. breast cancer patients. For the mRNA expression levels of the eight genes, Tables 5 and 6 present population-level marginal summaries of various estimands of the group potential outcomes for the concordant, combined, and MGO target populations. The inference procedure is described in Section 2.2. For example, for the lth biomarker, the group-specific mean $\mu_l^{(z)}$ and standard deviation $\sigma^{(z)}$ were estimated assuming $\boldsymbol{h}(\mathbf{y}) = (y_l, y_l^2)'$ in Theorem 2.1 and $\pi(t_1, t_2) = \sqrt{t_2 - t_1^2}$ in Corollary 2.1.2. Median $M_l^{(z)}$ was estimated by first estimating the CDF of potential outcome $Y_l^{(z)}$ for a fine grid of points. Group comparison estimands like $\mu_l^{(1)} - \mu_l^{(2)}$ (i.e., ATE) and $\sigma^{(1)}/\sigma^{(2)}$ were estimated by applying appropriately defined functionals to estimates of $\mu_l^{(1)}$, $\mu_l^{(2)}$, $\sigma_l^{(1)}$, and $\sigma_l^{(2)}$. The estimate and 95% confidence interval based on $B = 100$ bootstrap samples are displayed for each feature (row), target population (column), and gene (block) of Tables 5 and 6. For each gene-estimand combination, a confidence interval for the combined or MGO target population is marked in bold when the concordant target population's confidence interval is *narrower*.

Although the three target populations produced somewhat comparable results, we find that concordant target population provided the most accurate inferences, i.e., narrowest confidence intervals, for most gene-estimand combinations. For the concordant target population, the average potential outcomes of the genes CXCL12, IGF1, LEF1, PRB2, and SMR3B were significantly different for the two disease subtypes because the corresponding ATE confidence intervals did not include 0. For gene PRB2, the estimated ratio $\sigma_l^{(1)}/\sigma_l^{(2)}$

was much larger than 1 for all the bootstrap samples and are not shown in Table 6; the results overwhelmingly indicated that the standard deviation of the IDC and IDL potential outcomes are different. Additionally, we conclude that the standard deviation of the group-specific potential outcomes of genes COL9A3 and IVL are significantly different because the respective confidence intervals for estimand $\sigma_l^{(1)}/\sigma_l^{(2)}$ did not include 1. The group-specific medians may also be compared if required via $M_l^{(1)}/M_l^{(2)}$ or $M_l^{(1)} - M_l^{(2)}$.

The correlation between the potential outcomes of the l_1th and l_2th biomarker in the zth group was estimated as follows. For an M-variate function $\boldsymbol{h}(\mathbf{y}) = (h_1(\mathbf{y}), h_2(\mathbf{y}), h_3(\mathbf{y}))'$, where $M = 3$ and $\mathbf{y} \in \mathcal{R}^8$, we set the components $h_1(\mathbf{y}) = y_{l_1}$, $h_2(\mathbf{y}) = y_{l_3}$, $h_3(\mathbf{y}) = y_{l_1} y_{l_2}$. For group z, we estimated mean vector $\boldsymbol{\mu}^{(z)} = \left(\mathbb{E}[Y_{l_1}^{(z)}]_*, \mathbb{E}[Y_{l_2}^{(z)}]_*, \mathbb{E}[Y_{l_1}^{(z)} Y_{l_2}^{(z)}]_*\right)'$ for a target population by applying Theorem 2.1. Then, defining $\pi(t_1, t_2, t_3) = t_3 - t_1 t_2$, we applied Corollary 2.1.2 to infer the target population covariance, $\pi(\boldsymbol{\mu}^{(z)}) = \text{cov}(Y_{l_1}^{(z)}, Y_{l_2}^{(z)})_*$. Finally, using the previously estimated standard deviations $\sigma_{l_1}^{(z)}$ and $\sigma_{l_2}^{(z)}$ for the target population, we obtained the estimated correlation. Estimates from $B = 100$ bootstrap samples were used to construct 95% confidence intervals. For a target population, the true correlation between the l_1th and l_2th gene pair in the zth group of patients was declared significantly different from 0 using the 95% bootstrap confidence interval.

For every group and target population, Tables I–III of the Appendix present the full set of 95% confidence intervals of mRNA expression level correlation between each pair of genes. For the three target populations and two disease subtypes (groups), Table 7 lists the gene pairs that were significantly correlated within each group of patients. For concordant weights and disease subtype IDC, we find that gene CXCL12 was significantly co-expressed with the genes IGF1, ITGA11, and LEF1; gene IGF1 was co-expressed with ITGA11 and LEF1; gene COL9A3 was co-expressed with LEF1 and PRB2; and gene LEF1 was co-expressed with the genes IVL and ITGA11. For disease subtype ILC, only the CXCL12 - IGF1 gene pair was significantly associated. Consequently, the *differential correlation pat-*

COL9A3 ($l = 1$)			
Estimand	**Concordant**	**Combined**	**MGO**
$\mu_l{}^{(1)}$	-0.05 $(-0.27, 0.23)$	-0.11 $(\mathbf{-0.33, 0.21})$	-0.09 $(-0.25, 0.22)$
$\mu_l{}^{(2)}$	-0.11 $(-0.36, 0.20)$	-0.16 $(\mathbf{-0.44, 0.21})$	-0.19 $(\mathbf{-0.49, 0.27})$
$\sigma_l{}^{(1)}$	1.03 $(0.87, 1.26)$	0.97 $(\mathbf{0.84, 1.31})$	0.93 $(\mathbf{0.83, 1.36})$
$\sigma_l{}^{(2)}$	0.68 $(0.54, 0.86)$	0.69 $(\mathbf{0.47, 0.90})$	0.69 $(\mathbf{0.49, 0.91})$
$\mathrm{M}_l^{(1)}$	-0.19 $(-0.47, 0.07)$	-0.23 $(\mathbf{-0.46, 0.13})$	-0.23 $(-0.40, 0.11)$
$\mathrm{M}_l^{(2)}$	-0.05 $(-0.52, 0.37)$	0.07 $(\mathbf{-0.57, 0.49})$	-0.05 $(\mathbf{-0.54, 0.48})$
$\mu_l^{(1)} - \mu_l^{(2)}$	0.06 $(-0.33, 0.43)$	0.05 $(\mathbf{-0.48, 0.54})$	0.09 $(\mathbf{-0.36, 0.59})$
$\sigma_l^{(1)}/\sigma_l^{(2)}$	1.52 $(1.15, 2.09)$	1.41 $(\mathbf{1.11, 2.24})$	1.35 $(\mathbf{1.09, 2.24})$
CXCL12 ($l = 2$)			
Estimand	**Concordant**	**Combined**	**MGO**
$\mu_l{}^{(1)}$	-0.03 $(-0.22, 0.21)$	-0.03 $(\mathbf{-0.23, 0.29})$	0.02 $(\mathbf{-0.31, 0.22})$
$\mu_l{}^{(2)}$	0.59 $(0.23, 0.88)$	0.55 $(\mathbf{0.11, 1.01})$	0.58 $(\mathbf{0.26, 1.01})$
$\sigma_l{}^{(1)}$	0.91 $(0.84, 1.16)$	0.97 $(\mathbf{0.84, 1.21})$	0.94 $(\mathbf{0.83, 1.21})$
$\sigma_l{}^{(2)}$	0.80 $(0.52, 1.10)$	0.83 $(\mathbf{0.49, 1.27})$	0.82 $(\mathbf{0.54, 1.20})$
$\mathrm{M}_l^{(1)}$	-0.15 $(-0.20, 0.36)$	-0.16 $(\mathbf{-0.32, 0.36})$	-0.09 $(\mathbf{-0.35, 0.38})$
$\mathrm{M}_l^{(2)}$	0.68 $(0.44, 1.01)$	0.69 $(\mathbf{0.10, 1.16})$	0.58 $(\mathbf{0.21, 1.08})$
$\mu_l^{(1)} - \mu_l^{(2)}$	-0.62 $(-1.00, -0.12)$	-0.58 $(\mathbf{-1.18, -0.08})$	-0.56 $(\mathbf{-1.08, -0.17})$
$\sigma_l^{(1)}/\sigma_l^{(2)}$	1.14 $(0.87, 1.99)$	1.17 $(\mathbf{0.71, 2.32})$	1.14 $(\mathbf{0.75, 1.94})$
IGF1 ($l = 3$)			
Estimand	**Concordant**	**Combined**	**MGO**
$\mu_l{}^{(1)}$	0.04 $(-0.21, 0.23)$	0.10 $(\mathbf{-0.28, 0.31})$	0.13 $(\mathbf{-0.30, 0.30})$
$\mu_l{}^{(2)}$	0.82 $(0.54, 1.09)$	0.84 $(\mathbf{0.52, 1.16})$	0.82 $(\mathbf{0.52, 1.17})$
$\sigma_l{}^{(1)}$	0.81 $(0.80, 1.12)$	0.86 $(\mathbf{0.78, 1.18})$	0.87 $(\mathbf{0.75, 1.16})$
$\sigma_l{}^{(2)}$	0.76 $(0.47, 0.95)$	0.82 $(\mathbf{0.45, 1.13})$	0.76 $(\mathbf{0.45, 1.02})$
$\mathrm{M}_l^{(1)}$	-0.01 $(-0.18, 0.34)$	0.06 $(\mathbf{-0.23, 0.47})$	0.10 $(\mathbf{-0.26, 0.45})$
$\mathrm{M}_l^{(2)}$	0.95 $(0.60, 1.22)$	0.95 $(\mathbf{0.43, 1.28})$	0.88 $(\mathbf{0.52, 1.32})$
$\mu_l^{(1)} - \mu_l^{(2)}$	-0.77 $(-1.22, -0.43)$	-0.74 $(\mathbf{-1.19, -0.33})$	-0.69 $(\mathbf{-1.18, -0.31})$
$\sigma_l^{(1)}/\sigma_l^{(2)}$	1.06 $(0.94, 2.03)$	1.05 $(\mathbf{0.83, 2.33})$	1.14 $(\mathbf{0.82, 2.26})$
ITGA11 ($l = 4$)			
Estimand	**Concordant**	**Combined**	**MGO**
$\mu_l{}^{(1)}$	0.01 $(-0.28, 0.22)$	0.03 $(\mathbf{-0.37, 0.24})$	0.07 $(-0.29, 0.17)$
$\mu_l{}^{(2)}$	0.01 $(-0.48, 0.26)$	-0.02 $(\mathbf{-0.53, 0.27})$	0.07 $(\mathbf{-0.63, 0.28})$
$\sigma_l{}^{(1)}$	0.92 $(0.83, 1.10)$	0.96 $(\mathbf{0.80, 1.16})$	0.94 $(\mathbf{0.83, 1.19})$
$\sigma_l{}^{(2)}$	0.81 $(0.60, 1.03)$	0.93 $(\mathbf{0.54, 1.07})$	0.98 $(\mathbf{0.56, 1.15})$
$\mathrm{M}_l^{(1)}$	0.14 $(-0.28, 0.41)$	0.19 $(\mathbf{-0.49, 0.48})$	0.20 $(\mathbf{-0.36, 0.39})$
$\mathrm{M}_l^{(2)}$	-0.02 $(-0.54, 0.32)$	-0.22 $(\mathbf{-0.72, 0.26})$	-0.09 $(\mathbf{-0.55, 0.35})$
$\mu_l^{(1)} - \mu_l^{(2)}$	0.01 $(-0.28, 0.49)$	0.05 $(\mathbf{-0.41, 0.56})$	0.00 $(\mathbf{-0.44, 0.60})$
$\sigma_l^{(1)}/\sigma_l^{(2)}$	1.14 $(0.89, 1.62)$	1.03 $(\mathbf{0.86, 2.01})$	0.96 $(\mathbf{0.82, 1.84})$

Table 5: For four targeted genes, estimates and 95% bootstrap confidence levels (shown in parenthesis) of different population-level estimands of the potential outcomes of group 1 (IDC cancer subtype, denoted by superscript 1) and group 2 (ILC cancer subtype, denoted by superscript 2) with concordant, combined, and MGO weights. A combined or MGO confidence interval is highlighted in bold if it is *wider* than the concordant confidence interval. All numbers are rounded to 2 decimal places. See Section 4 for further explanation.

IVL ($l = 5$)			
Estimand	**Concordant**	**Combined**	**MGO**
$\mu_l{}^{(1)}$	-0.45 $(-0.56, -0.10)$	-0.48 $(\mathbf{-0.63, -0.07})$	-0.45 $(\mathbf{-0.63, -0.05})$
$\mu_l{}^{(2)}$	-0.61 $(-0.88, -0.39)$	-0.36 $(\mathbf{-0.90, -0.23})$	-0.37 $(\mathbf{-0.90, -0.28})$
$\sigma_l{}^{(1)}$	0.88 $(0.81, 1.19)$	0.85 $(\mathbf{0.73, 1.29})$	0.88 $(\mathbf{0.70, 1.23})$
$\sigma_l{}^{(2)}$	0.70 $(0.34, 0.96)$	0.90 $(\mathbf{0.29, 1.04})$	0.91 $(\mathbf{0.31, 1.03})$
$\mathrm{M}_l^{(1)}$	-0.78 $(-0.96, -0.40)$	-0.78 $(\mathbf{-1.01, -0.34})$	-0.78 $(\mathbf{-0.95, -0.38})$
$\mathrm{M}_l^{(2)}$	-0.89 $(-1.13, -0.56)$	-0.72 $(\mathbf{-1.13, -0.40})$	-0.75 $(\mathbf{-1.13, -0.47})$
$\mu_l^{(1)} - \mu_l^{(2)}$	0.16 $(-0.08, 0.64)$	-0.12 $(\mathbf{-0.25, 0.66})$	-0.08 $(\mathbf{-0.22, 0.74})$
$\sigma_l^{(1)}/\sigma_l^{(2)}$	1.26 $(1.00, 3.21)$	0.95 $(\mathbf{0.87, 3.36})$	0.96 $(\mathbf{0.86, 3.45})$
LEF1 ($l = 6$)			
Estimand	**Concordant**	**Combined**	**MGO**
$\mu_l{}^{(1)}$	-0.02 $(-0.21, 0.21)$	-0.01 $(\mathbf{-0.28, 0.25})$	0.04 $(-0.21, 0.20)$
$\mu_l{}^{(2)}$	0.33 $(-0.00, 0.68)$	0.28 $(\mathbf{-0.30, 0.68})$	0.35 $(\mathbf{-0.14, 0.74})$
$\sigma_l{}^{(1)}$	0.93 $(0.77, 1.18)$	0.90 $(0.81, 1.17)$	0.93 $(0.80, 1.15)$
$\sigma_l{}^{(2)}$	0.72 $(0.54, 1.11)$	0.61 $(\mathbf{0.53, 1.13})$	0.66 $(0.53, 1.07)$
$\mathrm{M}_l^{(1)}$	-0.10 $(-0.33, 0.16)$	-0.05 $(\mathbf{-0.38, 0.14})$	-0.03 $(\mathbf{-0.38, 0.16})$
$\mathrm{M}_l^{(2)}$	0.22 $(-0.09, 0.62)$	0.20 $(\mathbf{-0.22, 0.75})$	0.24 $(\mathbf{-0.17, 0.72})$
$\mu_l^{(1)} - \mu_l^{(2)}$	-0.35 $(-0.65, 0.07)$	-0.29 $(\mathbf{-0.79, 0.46})$	-0.31 $(\mathbf{-0.78, 0.23})$
$\sigma_l^{(1)}/\sigma_l^{(2)}$	1.29 $(0.91, 1.98)$	1.47 $(\mathbf{0.86, 1.90})$	1.41 $(\mathbf{0.85, 1.88})$
PRB2 ($l = 7$)			
Estimand	**Concordant**	**Combined**	**MGO**
$\mu_l{}^{(1)}$	-0.82 $(-0.88, -0.69)$	-0.83 $(\mathbf{-0.90, -0.66})$	-0.84 $(\mathbf{-0.89, -0.65})$
$\mu_l{}^{(2)}$	-0.88 $(-0.95, -0.50)$	-0.87 $(\mathbf{-0.95, -0.04})$	-0.89 $(\mathbf{-0.95, -0.31})$
$\sigma_l{}^{(1)}$	0.38 $(0.20, 0.79)$	0.41 $(\mathbf{0.21, 0.94})$	0.40 $(\mathbf{0.22, 0.95})$
$\sigma_l{}^{(2)}$	0.19 $(0.00, 1.48)$	0.23 $(\mathbf{0.00, 2.08})$	0.20 $(\mathbf{0.00, 1.82})$
$\mathrm{M}_l^{(1)}$	-0.95 $(-0.95, -0.95)$	-0.95 $(-0.95, -0.95)$	-0.95 $(-0.95, -0.95)$
$\mathrm{M}_l^{(2)}$	-0.95 $(-0.95, -0.95)$	-0.95 $(-0.95, -0.95)$	-0.95 $(-0.95, -0.95)$
$\mu_l^{(1)} - \mu_l^{(2)}$	0.06 $(-0.30, 0.21)$	0.04 $(-0.80, 0.29)$	0.05 $(-0.50, 0.28)$
SMR3B ($l = 8$)			
Estimand	**Concordant**	**Combined**	**MGO**
$\mu_l{}^{(1)}$	-0.65 $(-0.78, -0.40)$	-0.69 $(\mathbf{-0.79, -0.19})$	-0.67 $(\mathbf{-0.77, -0.26})$
$\mu_l{}^{(2)}$	0.04 $(-0.50, 0.29)$	-0.04 $(\mathbf{-0.57, 0.39})$	-0.11 $(\mathbf{-0.60, 0.41})$
$\sigma_l{}^{(1)}$	0.68 $(0.36, 1.15)$	0.65 $(\mathbf{0.31, 1.48})$	0.68 $(\mathbf{0.36, 1.42})$
$\sigma_l{}^{(2)}$	1.01 $(0.68, 1.26)$	1.05 $(\mathbf{0.54, 1.28})$	1.02 $(\mathbf{0.58, 1.32})$
$\mathrm{M}_l^{(1)}$	-0.94 $(-0.94, -0.94)$	-0.94 $(\mathbf{-0.94, -0.86})$	-0.94 $(-0.94, -0.94)$
$\mathrm{M}_l^{(2)}$	-0.25 $(-0.94, 0.06)$	-0.25 $(\mathbf{-0.94, 0.42})$	-0.57 $(\mathbf{-0.94, 0.26})$
$\mu_l^{(1)} - \mu_l^{(2)}$	-0.70 $(-0.88, -0.15)$	-0.65 $(\mathbf{-1.07, 0.07})$	-0.56 $(\mathbf{-1.11, 0.02})$
$\sigma_l^{(1)}/\sigma_l^{(2)}$	0.67 $(0.38, 1.38)$	0.61 $(\mathbf{0.36, 1.80})$	0.66 $(\mathbf{0.37, 1.70})$

Table 6: For four targeted genes, estimates and 95% bootstrap confidence levels (shown in parenthesis) of different population-level estimands of the potential outcomes of group 1 (IDC cancer subtype, denoted by superscript 1) and group 2 (ILC cancer subtype, denoted by superscript 2) with concordant, combined, and MGO weights. A combined or MGO confidence interval is highlighted in bold if it is *wider* than the concordant confidence interval. All numbers are rounded to 2 decimal places. See Section 4 for further explanation.

Infiltrating Ductal Carcinoma	
Target population	**Significantly correlated gene pairs**
Concordant	CXCL12-IGF1, CXCL12-ITGA11, IGF1-ITGA11, COL9A3-LEF1, CXCL12-LEF1, IGF1-LEF1, ITGA11-LEF1, IVL-LEF1, COL9A3-PRB2
Combined	CXCL12-IGF1, CXCL12-ITGA11, IGF1-ITGA11, CXCL12-LEF1, IGF1-LEF1, COL9A3-PRB2
MGO	CXCL12-IGF1, CXCL12-ITGA11, IGF1-ITGA11, CXCL12-LEF1, IGF1-LEF1, COL9A3-PRB2
Infiltrating Lobular Carcinoma	
Target population	**Significantly correlated gene pairs**
Concordant	CXCL12-IGF1
Combined	CXCL12-IGF1
MGO	CXCL12-IGF1

Table 7: Significantly correlated pairs of genes for each target population and disease subtype.

tern for the concordant target population consisted of the gene pairs (CXCL12, ITGA11), (IGF1, ITGA11), (COL9A3, LEF1), (CXCL12, LEF1), (IGF1, LEF1), (ITGA11, LEF1), (IVL, LEF1), and (COL9A3, PRB2).

By contrast, the combined and MGO target populations detected identical differential correlation patterns comprising 5 gene pairs. These biomarkers are cataloged in Table 7 and were also detected by the concordant population. However, unlike the concordant weights, the competing methods did not find any association between group membership and the gene pairs (COL9A3, LEF1), (ITGA11, LEF1), and (IVL, LEF1). Figure 1 summarizes the many-way relationships between the differentially correlated sets of gene pairs discovered by the weighting methods and (biased) unadjusted analyses.

Recent literature on breast cancer gene ontology supports the distinctive findings of the concordant weighting method. For example, Williams et al. (2022) reported that the

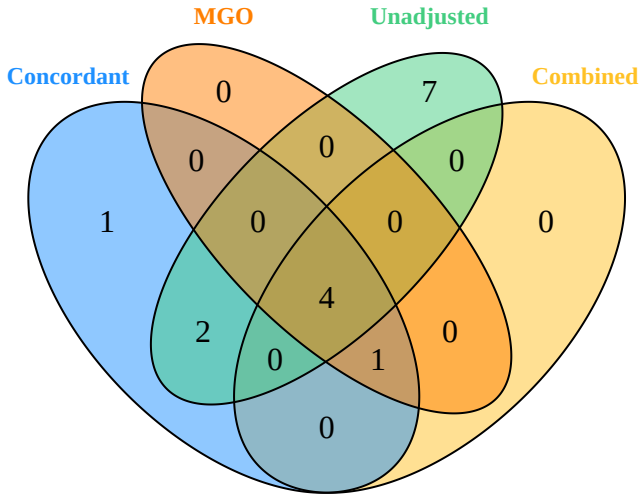

Figure 1: Venn diagram of the differential correlation pattern of targeted gene pairs for the three target populations and unadjusted analysis.

genes IVL and LEF1 are highly expressed in basal and metaplastic human breast cancers. In an analysis of advanced stage breast cancer tumors, Malvia et al. (2019) discovered the deregulation of the cell adhesion and ECM receptor pathways, as well as pathways in cancer, to which genes TGA11 and LEF1 belong. Paul (2020) showed that breast cancer metastases harbored mutations within the WNT signaling gene set, affecting downstream the focal adhesion and cell cycle pathways containing genes COL9A3 and LEF1.

5 Discussion

While meta-analyzing observational studies, general inference procedures for uncensored continuous, categorical, or multivariate subject outcomes are often inadequate, especially when the inferential goals prioritize estimands other than ATE, ATT and ATO. This paper proposes new unconfounded weighted estimators for various population-level marginal features and estimands related to group comparisons. We evaluate asymptotic properties of

the proposed estimators and devise bootstrap procedures for uncertainty estimation. The techniques are broadly applicable to different weighting methods, including the estimand-agnostic concordant weights of Guha et al. (2022). Through simulation studies and data analyses, we exhibit the effectiveness of the concordant target population with univariate and multivariate study endpoints and various kinds of estimands. However, despite the methodological advances of this work, weighting approaches are increasingly challenged and rendered ineffectual by high-dimensional covariates. Our future research will meet these challenges by formulating extensions of the concordant weighting strategy.

Funding

This work was supported by the National Science Foundation under award DMS-1854003 to SG, and by the National Institutes of Health under award CA269398 to SG, awards CA269398, CA209414, and CA249096 to YL, and awards CA269398, CA209414, HL060710, and ES000002 to DCC, and award CA269398 to SVS.

References

Austin, P. C. (2010), 'The performance of different propensity-score methods for estimating differences in proportions (risk differences or absolute risk reductions) in observational studies', *Statistics in Medicine* **29**(20), 2137–2148.

Bickel, P. J. & Freedman, D. A. (1981), 'Some asymptotic theory for the Bootstrap', *The Annals of Statistics* **9**(6), 1196 – 1217.

Christopoulos, P. F., Msaouel, P. & Koutsilieris, M. (2015), 'The role of the insulin-like growth factor-1 system in breast cancer', *Molecular Cancer* **14**(1), 1–14.

Crump, R. K., Hotz, V. J., Imbens, G. W. & Mitnik, O. A. (2006), Moving the goalposts: addressing limited overlap in the estimation of average treatment effects by changing the estimand, Technical report, National Bureau of Economic Research.

Donzelli, S., Sacconi, A., Turco, C., Gallo, E., Milano, E., Iosue, I., Blandino, G., Fazi, F. & Fontemaggi, G. (2020), 'Paracrine signaling from breast cancer cells causes activation of id4 expression in tumor-associated macrophages', *Cells* **9**(2), 418.

Efron, B. & Tibshirani, R. J. (1994), *An introduction to the Bootstrap*, CRC press.

Feng, Y., Spezia, M., Huang, S., Yuan, C., Zeng, Z., Zhang, L., Ji, X., Liu, W., Huang, B., Luo, W. et al. (2018), 'Breast cancer development and progression: Risk factors, cancer stem cells, signaling pathways, genomics, and molecular pathogenesis', *Genes & Diseases* **5**(2), 77–106.

Guha, S., Christiani, D. C. & Li, Y. (2022), 'A new integrative method for multigroup comparisons of censored survival outcomes in multiple observational studies'.
URL: *https://arxiv.org/abs/2209.06361*

Hirano, K. & Imbens, G. W. (2001), 'Estimation of causal effects using propensity score weighting: an application to data on right heart catheterization', *Health Services and Outcomes Research Methodology* **2**(3), 259–278.

Imbens, G. W. (2000), 'The role of the propensity score in estimating dose-response functions', *Biometrika* **87**(3), 706–710.

Johnson, R. A., Wichern, D. W. et al. (2002), *Applied multivariate statistical analysis*, Vol. 5, Prentice hall Upper Saddle River, NJ.

Kumar, B., Chand, V., Ram, A., Usmani, D. & Muhammad, N. (2020), 'Oncogenic muta-

tions in tumorigenesis and targeted therapy in breast cancer', *Current Molecular Biology Reports* **6**(3), 116–125.

Li, F. & Li, F. (2019), 'Propensity score weighting for causal inference with multiple treatments', *The Annals of Applied Statistics* **13**(4), 2389–2415.

Li, F., Morgan, K. L. & Zaslavsky, A. M. (2018), 'Balancing covariates via propensity score weighting', *Journal of the American Statistical Association* **113**(521), 390–400.

Li, L. & Greene, T. (2013), 'A weighting analogue to pair matching in propensity score analysis', *The International Journal of Biostatistics* **9**(2), 215–234.

Lunceford, J. K. & Davidian, M. (2004), 'Stratification and weighting via the propensity score in estimation of causal treatment effects: a comparative study', *Statistics in Medicine* **23**(19), 2937–2960.

Malvia, S., Bagadi, S. A. R., Pradhan, D., Chintamani, C., Bhatnagar, A., Arora, D., Sarin, R. & Saxena, S. (2019), 'Study of gene expression profiles of breast cancers in indian women', *Scientific Reports* **9**(1), 1–15.

NCI (2022), 'Genomic data commons data portal'. https://portal.gdc.cancer.gov/.

Paul, M. R. (2020), The Genomic Evolution of Breast Cancer Metastasis, PhD thesis, University of Pennsylvania.

Robins, J. M., Hernan, M. A. & Brumback, B. (2000), 'Marginal structural models and causal inference in epidemiology', *Epidemiology* **11**(5), 550–560.

Robins, J. M. & Rotnitzky, A. (1995), 'Semiparametric efficiency in multivariate regression models with missing data', *Journal of the American Statistical Association* **90**(429), 122–129.

Rosenbaum, P. R. & Rubin, D. B. (1983), 'The central role of the propensity score in observational studies for causal effects', *Biometrika* **70**(1), 41–55.

Rubin, D. B. (2007), 'The design versus the analysis of observational studies for causal effects: parallels with the design of randomized trials', *Statistics in Medicine* **26**, 20–36.

Singh, K. (1981), 'On the asymptotic accuracy of Efron's bootstrap', *The Annals of Statistics* **9**(6), 1187–1195.

Tran, H.-T. (2022), 'Invasive lobular carcinoma'. https://www.hopkinsmedicine.org/health/conditions-and-diseases/breast-cancer/invasive-lobular-carcinoma.

Van der Vaart, A. W. (2000), *Asymptotic Statistics*, Cambridge University Press.

Wang, C. & Rosner, G. L. (2019), 'A Bayesian nonparametric causal inference model for synthesizing randomized clinical trial and real-world evidence', *Statistics in Medicine* **38**(14), 2573–2588.

Williams, R., Jobling, S., Sims, A. H., Mou, C., Wilkinson, L., Collu, G. M., Streuli, C. H., Gilmore, A. P., Headon, D. J. & Brennan, K. (2022), 'Elevated edar signalling promotes mammary gland tumourigenesis with squamous metaplasia', *Oncogene* **41**(7), 1040–1049.

Wright, P. (2022), 'Invasive ductal carcinoma (idc)'. https://www.hopkinsmedicine.org/health/conditions-and-diseases/breast-cancer/invasive-ductal-carcinoma-idc.

Zielińska, K. A. & Katanaev, V. L. (2020), 'The signaling duo cxcl12 and cxcr4: Chemokine fuel for breast cancer tumorigenesis', *Cancers* **12**(10), 3071.